Efficient elimination of microbial infections in wounds using plasma-activated water hydrogel

Debapriya Mukherjee[1#], Pallab Ghosh[1#], Raju S Rajmani[2], Kavita Verma[3], Akhil Gowda[3], Apoorva Birua[1], Lakshminarayana Rao*[3,4], Dipshikha Chakravortty*[1,5]

[1] Department of Microbiology and Cell Biology, Indian Institute of Science, Bangalore, India

[2] Centre for Infectious Disease Research, Indian Institute of Science, Bangalore, India

[3] Centre for Sustainable Technologies, Indian Institute of Science, Bangalore, India

[4]Interdisciplinary Centre for Water Research, Indian Institute of Science, Bangalore, India

[5] School of Biology, Indian Institute of Science Education and Research, Thiruvananthapuram, India

# Equal contribution

* Corresponding Authors

Lakshminarayana Rao, Centre for Sustainable Technologies, Indian Institute of Science, Bangalore, Karnataka 560012, India.

Email: narayana@iisc.ac.in

Dipshikha Chakravortty, Department of Microbiology and Cell Biology, Indian Institute of Science, Bangalore, Karnataka 560012, India.

Email: dipa@iisc.ac.in

Abstract

Surgical site infections are among the most prevalent postoperative complications and remain a pressing global health challenge, exacerbated by the rise of antimicrobial resistance. Plasma-activated water (PAW) has recently gained attention as an innovative antimicrobial approach. However, earlier research indicated that its effectiveness relies on maintaining an acidic pH. To address this, we previously created a high-strength, neutral pH–buffered version (hs-PAbW) that is better suited for clinical use in humans. This neutral plasma activated water retained the potent antimicrobial activity. In this study, we engineered a hydrogel containing hs-PAbW at a bactericidal yet non-cytotoxic dose (hs-PAbW-20) and assessed its efficacy in murine wound models. In Balb/c mice, hs-PAbW-20 gel significantly reduced *Pseudomonas aeruginosa* and *Staphylococcus aureus* burden, achieving results comparable to neomycin and soframycin treatments. This gel also accelerated wound closure by modulating genes crucial for wound repair. In diabetic C57BL/6 mouse model, hs-PAbW-20 gel decreased the burden of *P. aeruginosa* and promoted faster healing. Together, these findings establish hs-PAbW-20 gel as a promising next-generation therapeutic with the potential to overcome limitations of conventional antibiotic-based wound care.

Keywords: PAW, hs-PAbW-20, wound infections, wound healing, diabetic wound

43 ## Introduction

44 Surgical site infections (SSIs) are among the most common postoperative complications and a
45 major global health concern (1). Defined as infections occurring within 30 days of surgery, or
46 within one year with implants, they arise from both external sources (e.g., the surgical
47 environment) and internal sources (e.g., skin flora or exposed viscera). According to CDC
48 NNIS data, SSIs are the third most frequent hospital-acquired infection, representing 14–16%
49 of all cases and 38% in surgical patients, leading to increased morbidity, mortality, and
50 healthcare costs (2-4).

51 Multiple pathogens are implicated in SSIs, with *Staphylococcus aureus*, *Pseudomonas*
52 *aeruginosa*, *Klebsiella pneumoniae*, and *Acinetobacter baumannii* being most common (5-8).
53 Standard antimicrobial therapies are increasingly compromised by antibiotic resistance. In
54 Indian context, 62.27% of *S. aureus* isolates in Mysuru were methicillin-resistant, while 84.7%
55 of *P. aeruginosa* isolates in Southern Odisha were multidrug-resistant and 35.7% extensively
56 drug-resistant (9, 10). These resistance patterns emphasize the urgent need for alternatives to
57 conventional antibiotics.

58 An emerging antimicrobial approach is plasma-activated water (PAW), generated by exposing
59 water to cold plasma, an ionized gas containing electrons, ions, and neutral atoms (11-13).
60 Plasma–water interactions produce reactive oxygen (ROS) and nitrogen species (RNS), which
61 confer antimicrobial activity (14-16). Traditional PAW formulations depend on acidic pH for
62 reactivity, however, previous studies from our group demonstrated the generation of high
63 strength buffered PAW (hs-PAbW) at neutral pH, where antimicrobial effects in ESKAPE
64 pathogens are mediated through RNS-driven peroxynitrite formation and nitrotyrosine
65 generation (17-20).

In this study, we combined hs-PAbW with a hydrogel matrix to develop a non-toxic antimicrobial formulation and evaluated its potential in clearing wound infections. This composite demonstrated enhanced clearance of *P. aeruginosa* and *S. aureus* from wounds and accelerated wound closure, with outcomes comparable or superior to standard topical antibiotics. Our findings establish hs-PAbW hydrogel as a promising antibiotic alternative for wound management in the era of escalating antimicrobial resistance.

Materials and methods

Generation of hs-PAbW-20 hydrogel

The hs-PAbW was produced following a previously reported protocol (17, 19, 20). It was generated by applying a 10 kV, 20 kHz AC plasma discharge inside a 100 ml glass vessel equipped with aluminium electrodes, treating 50 ml of solution for 60 minutes, and repeating the process at least three times. The setup used 25 mM bicarbonate water with 1 LPM air bubbling and a 5 mm discharge gap, consuming 32 ± 2 W. To obtain 20% of the hs-PAbW strength, the solution was diluted at a 1:5 ratio in 25 mM bicarbonate water. Additionally, 0.5% edible grade xanthan powder was added as a gelling agent to prepare the hs-PAbW-20 gel.

Bacterial strains and culture conditions

Methicillin-resistant *Staphylococcus aureus* (Isolate-SA3) was kindly provided by Prof. Pradyut Prakash, Banaras Hindu University, India. *Pseudomonas aeruginosa* (PAO1) was generously supplied by Prof. Anne-Béatrice Blanc-Potard, Université de Montpellier. The bacterial strains were revived on Luria-Bertani (LB) agar plates (HiMedia) from glycerol stocks stored at −80 °C. A single colony was then inoculated into LB broth (HiMedia) and

89 cultured overnight at 37 °C in a shaking incubator set to 170 rpm to obtain the stationary phase.
90 The overnight culture was subcultured at a ratio of 1:100 and incubated under the same
91 conditions for 6 hours to obtain the logarithmic phase culture.

92

93 **Propidium Iodide staining**

94 Propidium iodide staining was carried out using a protocol adapted with minor modifications
95 from Roy Chowdhury *et al.* and Mukherjee *et al* (20-22). In brief, cultures of *P. aeruginosa*
96 and *S. aureus* were incubated with 100 µl of hs-PAbW-gel for 16 hours at 37 °C under static
97 conditions. The bacterial cells were then stained with propidium iodide (Sigma) at a final
98 concentration of 1 µg/mL. Flow cytometry analysis was performed using a BD FACSVerse
99 (BD Biosciences), and the data were processed with BD FACSuite software.

100

101 **Eukaryotic cell lines and growth conditions**

102 The L929 mouse fibroblast cell line (ATCC) was maintained in Dulbecco's Modified Eagle's
103 Medium (DMEM, Sigma-Aldrich) supplemented with 10% fetal calf serum (FCS, Gibco) and
104 incubated at 37 °C in a humidified atmosphere containing 5% CO_2.

105

106 ***In-vitro* cell migration assay**

107 The effect of hs-PAbW-20 gel on *in vitro* migration of L929 cells was evaluated following
108 previously described protocols (23, 24). In brief, 1×10^5 cells were seeded into 24-well plates
109 and cultured overnight. After washing with 1× phosphate-buffered saline (PBS), a scratch was
110 introduced using a sterile 200 µl pipette tip. Detached cells and debris were removed by
111 additional PBS washes. Cells were then treated with hs-PAbW-100 gel and control gel at a

volume equivalent to 1:5 of the total cell media volume and incubated for 24 hours. Cell migration at 0 h and 24 h was documented using mobile camera affixed to the microscope eyepiece. Scratch widths at both time points were quantified using ImageJ software.

Ethics statement for animal experiments

All animal studies were approved by the Institutional Animal Ethics Committee (IAEC) of the Indian Institute of Science, Bangalore (Registration No: 48/1999/CPCSEA). Experimental procedures were carried out in full compliance with the guidelines of the Committee for the Purpose of Control and Supervision of Experiments on Animals (CPCSEA). The ethical approval number for this work is CAF/Ethics/973/2023.

Wound healing experiment in mice

Wound healing experiments were performed by modifying a previously published protocol (25). BALB/c and C57BL/6 mice (10–12 weeks old) were anesthetized intravenously with ketamine hydrochloride (120 mg/kg). Following dorsal depilation, two full-thickness excisional wounds (10 mm in diameter) were created bilaterally along the midline using a sterile biopsy punch. Each wound was inoculated with either 10^5 CFU of *P. aeruginosa* or 10^4 CFU of *S. aureus* and allowed to incubate for 30 minutes to establish infection. Treatment was initiated on day 0 with hs-PAbW-20 gel, control gel, or the antibiotic creams neomycin and soframycin. Approximately 100 µl of either gel formulation (control or hs-PAbW-20) or antibiotic cream was applied to each wound on alternate days until day 7, with wound photographs taken throughout the treatment. On day 9, mice were euthanized, and wound tissues were collected for downstream analysis. Wound closure was assessed by measuring wound diameters using ImageJ software.

136

137 **Generation of diabetic mice model**

138 Type I diabetes mellitus was induced in 10–12-week-old male C57BL/6 mice using
139 streptozotocin (Sigma), following the protocol of Furman *et al* (26). Briefly, mice received
140 intraperitoneal injections of streptozotocin of 40 mg/kg for five consecutive days, after which
141 they were maintained for seven days on a standard chow diet. During the initial 5-day treatment
142 period, mice were provided with 10% sucrose water, which was replaced with normal drinking
143 water from day 6 onward. Blood glucose levels were measured before and after treatment using
144 a Dr. Morepen BG-03 Gluco One Glucometer. After the 7-day housing period, full-thickness
145 excisional wounds were created in the diabetic mice, inoculated with 10^4 CFU of *P. aeruginosa*,
146 subsequently treated with gels and antibiotic creams, and imaged as described previously.

147

148 **Bacterial burden enumeration by spread plating**

149 At 9 dpi, wound tissues were harvested in 1× PBS, homogenized using a bead beater, and the
150 resulting lysates were spread-plated onto selective agar plates at suitable dilutions. Plates were
151 incubated overnight at 37 °C under static conditions, after which colony-forming units (CFU)
152 were enumerated, corrected for dilution factors, and normalized to tissue weight to calculate
153 bacterial burden. Cetrimide agar (HiMedia) was used for *P. aeruginosa*, while mannitol salt
154 agar (HiMedia) was used for *S. aureus*.

155

156 **RNA Isolation and RT-qPCR**

157 At 9 dpi, wound tissues were collected in TRIzol (RNAiso Plus, TaKaRa) and stored at −80 °C
158 until further use. RNA was extracted using the phenol–chloroform method, and the final RNA

159 pellet was dissolved in 30 µl of DEPC-treated Milli-Q water. The samples were then subjected
160 to DNase treatment (Invitrogen TURBO™ DNase, AM2239), followed by cDNA synthesis
161 using the RevertAid First Strand cDNA Synthesis Kit (K1622). RT-qPCR was carried out with
162 SYBR Green chemistry (PowerUp™ SYBR™ Green Master Mix, A25742) on a QuantStudio
163 5 system. Gene expression levels were normalized to β-actin expression. The primers are
164 enlisted in **Table 1**.

165 **Table 1: List of primers**

Primer name	Sequence (5'-3')
Mouse *Pdgf-b* FP	TCTACCCGATGGCTCCTTCA
Mouse *Pdgf-b* RP	AAGGAAGCAGAAGGAACG
Mouse *Egfr* FP	TAACTCCAAAGGCCACCCAC
Mouse *Egfr* RP	AATCCGAGACAGACGGAGTC
Mouse *Mmp1* FP	CTGCTTTACTGCCAGCGTTC
Mouse *Mmp1* RP	TGGGAGAGGCCAATTAGGGA
Mouse *Mmp3* FP	AGGAGGCAGCAGAGAACCTA
Mouse *Mmp3* RP	GCAGAAGCTCCATACCAGCA
Mouse beta-actin FP	AGAAGAGCTATGAGCTGCCTGA
Mouse beta-actin RP	CAAGAAGGAAGGCTGGAAAAGAG

166

167 **Histopathology imaging**

168 Wound tissues were taken at 9 dpi and preserved in 3.5% paraformaldehyde. The samples were
169 outsourced for sectioning and staining with haematoxylin-eosin. Images were taken with a light
170 microscope and a veterinary doctor with experience in the field evaluated them for pathology.

171

172 **Statistical Analysis**

173 Biological and technical replicates for each experiment are noted in the figure legends.
174 Statistical analyses were performed using one-way ANOVA, two-way ANOVA, or the Mann-
175 Whitney U-test, as specified in the figure legends. A *p*-value of less than 0.05 was considered
176 statistically significant. Results are presented as the mean ± SD or mean ± SEM, with the
177 specific format also indicated in the figure legends. All bar graphs and statistical tests were
178 created and performed using GraphPad Prism 8.4.3 (686).

179

180 Results

181 **The hs-PAbW-20 gel maintained its antibacterial effectiveness while having no effect on**
182 **the migration of mouse fibroblast cells.**

183 In our earlier study, hs-PAbW was shown to be non-cytotoxic in L929 mouse fibroblast cells
184 when diluted at a 1:5 (v/v) ratio, while simultaneously reducing the bacterial load of *S. aureus*
185 compared to control water (20). In the present work, hs-PAbW was therefore diluted to one-
186 fifth of its original strength and combined with a gelling agent to develop the hs-PAbW-20 gel,
187 aiming to improve its practical usability.

188 Chronic wound infections caused by *P. aeruginosa* and *S. aureus* are highly prevalent among
189 hospitalized patients (27). To determine whether hs-PAbW-20 maintained its bactericidal
190 properties in the gel formulation and was effective against these two pathogens, logarithmic

191 phase cultures of *P. aeruginosa* and *S. aureus* (10^8 C.F.U each) were incubated with 100 µl of
192 hs-PAbW-20 overnight at 37°C. The significant rise in the percentage of propidium iodide (PI)-
193 positive cells and median fluorescence intensity (MFI), in comparison with the control gel,
194 confirmed that hs-PAbW-20 preserved its antimicrobial activity in the gel form (**Figure 1A-**
195 **C**).

196 Cell migration plays an essential role in processes such as development, wound repair, immune
197 function, and cancer progression/metastasis (28). A scratch assay performed on L929 cells
198 showed that treatment did not interfere with the normal reduction in scratch width after 24 h.
199 This indicates that cell migration remained unaffected when exposed to the plasma-activated
200 hydrogel. Collectively, these preliminary *in vitro* results demonstrated that hs-PAbW-20
201 hydrogel exhibited strong antimicrobial activity against *P. aeruginosa* and *S. aureus*, while also
202 preserving cell migration behaviour due to its non-cytotoxic nature.

203

204 **Use of hs-PAbW-20 gel led to a reduction in *P. aeruginosa* burden in infected wounds,**
205 **along with faster wound closure and elevated transcriptional expression of genes needed**
206 **for wound healing**

207 To evaluate wound healing and antimicrobial efficacy of hs-PAbW-20 gel, bilateral full-
208 thickness excisional wounds (10 mm) were created in 10–12-week-old male BALB/c mice and
209 infected with 10^5 CFU of *P. aeruginosa*. Wounds were treated with PBS, control gel, or hs-
210 PAbW-20 gel at 30 min, day 2, day 5, and day 7 post-infection, and closure was subsequently
211 monitored. Treatment of *P. aeruginosa*–infected wounds with hs-PAbW-20 gel resulted in a
212 significantly greater reduction in wound diameter relative to day 0 compared with PBS or
213 control gel (**Figure 2A–B**). This was accompanied by a significant decrease in bacterial burden

214 in hs-PAbW-20–treated samples than in PBS- or control gel–treated groups (**Figure 2C**),
215 confirming that hs-PAbW-20 gel retained antimicrobial activity *in vivo*.

216 Previous studies have highlighted the roles of matrix metalloproteinases (MMPs), epidermal
217 growth factors (EGF), and platelet-derived growth factor (PDGF) in wound healing (29-31).
218 Accordingly, we assessed mRNA levels of epidermal growth factor receptor (*Egfr*) and matrix
219 metalloproteinase 3 (*Mmp3*) in wound tissues under different treatments. Expression of both
220 *Egfr* and *Mmp3* was significantly upregulated in hs-PAbW-20–treated infected wounds
221 compared with other treatment groups and the uninfected control (**Figure 2D-E**).

222 To further examine the efficacy of hs-PAbW-20 gel in an additional mouse model, similar
223 experiments were performed in 10–12-week-old male C57BL/6 mice (**Figure S1**). In this
224 strain, wound closure following *P. aeruginosa* infection and treatment with hs-PAbW-20 gel
225 did not show a significant difference when compared with the control treatment groups (**Figure**
226 **S1A-B**). However, hs-PAbW-20 gel continued to display bactericidal activity in the C57BL/6
227 model, as indicated by a significant reduction in *P. aeruginosa* burden in the hs-PAbW-20–
228 treated wounds relative to PBS- and control gel–treated wounds (**Figure S1C**). In addition, the
229 expression of wound healing–related markers such as *Pdgf*, *Egfr*, *Mmp1*, and *Mmp3* was
230 significantly upregulated in *P. aeruginosa*–infected wounds treated with hs-PAbW-20 gel
231 compared with both treatment controls and the uninfected control group (**Fig S2A-D**).
232 Collectively, these findings demonstrate that hs-PAbW-20 gel is effective in clearing bacterial
233 infection in wounds across both mouse models while also enhancing the expression of wound
234 healing genes. Nonetheless, the comparable wound closure observed in hs-PAbW-20–treated
235 C57BL/6 mice, despite reduced bacterial burden, may be attributed to genetic differences
236 between Balb/c and C57BL/6 strains, as the latter are characterized by a predominant Th1
237 immune response that promotes a more proinflammatory environment (32).

238

239 **The hs-PAbW-20 gel demonstrated efficacy comparable to that of commercially available**
240 **antibiotic creams in reducing *P. aeruginosa* loads in wounds in the *in vivo* model.**

241 Currently, antibacterial ointments such as neomycin and soframycin serve as the standard
242 regimen for managing wound infections. Building on our prior findings that demonstrated the
243 antibacterial and wound-healing capabilities of hs-PAbW-20 gel, we aimed to evaluate its
244 performance against these commercial ointments in resolving wound infections. For this study,
245 we induced infections in skin wounds of 10-12-week-old male BALB/c mice using 10^5 CFU
246 of *P. aeruginosa*, followed by treatment with neomycin, soframycin, a control gel, or hs-PAbW-
247 20 gel at specified intervals after infection, as detailed previously (**Figure 3**). Our results
248 showed that by 7 dpi, the fold decrease in wound diameter (relative to day 0) was markedly
249 greater in mice treated with hs-PAbW-20 gel than in those receiving the control gel or antibiotic
250 ointments (**Figure 3A-B**). Moreover, hs-PAbW-20 gel treatment achieved a comparable
251 bacterial load within the wounds to that seen with neomycin and soframycin, indicating
252 equivalent efficacy in eradicating the infection relative to these antibiotics (**Figure 3C**).
253 Additionally, expression levels of *Pdgf*, *Egfr*, and *Mmp1* were notably elevated in hs-PAbW-
254 20 gel-treated tissues, mirroring the upregulation observed in the soframycin group (**Figure**
255 **S3A-D**).

256 Histological examination of wound sections further supported these observations. In wounds
257 infected with *P. aeruginosa*, the control gel-treated groups exhibited severe pathology scores
258 of 4, characterized by necrotic epidermis, inadequate re-epithelialization, and disorganized
259 dermis in PBS samples, alongside persistent heavy inflammatory infiltrates. In contrast, hs-
260 PAbW-20 gel administration restored tissue architecture, yielding a pathology score of 2, which
261 is consistent with the scores from both antibiotic ointments (**Figure 4**). These findings from

262 histopathological assessment reinforce the effectiveness of hs-PAbW-20 gel as a potent wound-
263 healing therapeutic.

264

265 **hs-PAbW-20 gel effectively reduced *S. aureus* load in infected wounds, promoting**
266 **accelerated closure comparable to commercial antibiotic ointments.**

267 In addition to *P. aeruginosa*, *S. aureus* represents another prominent pathogen implicated in
268 wound infections (27). To assess the efficacy of hs-PAbW-20 gel in mitigating *S. aureus*
269 bacterial burden, we conducted parallel experiments using 10–12-week-old male BALB/c
270 mice. Open wounds were inoculated with *S. aureus* at day 0, followed by initiation of
271 treatments with control gel, hs-PAbW-20 gel, neomycin, or soframycin; applications were
272 administered every other day through day 7. Consistent with our prior findings for *P.*
273 *aeruginosa*, hs-PAbW-20 gel treatment elicited a greater decrease in wound diameter relative
274 to the control gel group, comparable to outcomes in cohorts receiving the commercial antibiotic
275 ointments (**Figure S4A–B**). Furthermore, hs-PAbW-20 gel substantially reduced *S. aureus*
276 colony-forming units in the wounds compared with the control gel, achieving a terminal
277 bacterial load equivalent to that observed in the neomycin-treated group (**Figure S4C**). hs-
278 PAbW-20 gel also enhanced transcriptional expression of the wound-healing markers *Pdgf*,
279 *Egfr*, and *Mmp1* in wound tissues, mirroring the elevations seen in neomycin- and soframycin-
280 treated samples (**Figure S5A–C**).

281 Haematoxylin and eosin staining of wound sections demonstrated that control gel treatment
282 yielded severe pathology, including disorganized dermis, necrotic epidermis, and impaired re-
283 epithelialization (pathology score of 4). In contrast, hs-PAbW-20 gel treatment lowered the
284 pathology score to 3 relative to control gel-treated groups. Neomycin and soframycin
285 treatments further ameliorated tissue damage, reducing pathology scores to 0 and 1,

286 respectively (**Figure S6**). Collectively, these results indicate that hs-PAbW-20 gel effectively
287 combats *S. aureus* wound infections, exhibiting efficacy broadly comparable to that of
288 neomycin and soframycin.

289

290 **hs-PAbW-20 gel effectively reduces bacterial burden in *P. aeruginosa*-infected wounds of**
291 **diabetic mice, along with improved wound closure**

292 Delayed wound healing is a major challenge in diabetic patients, as the wound environment
293 often favours bacterial colonization, further slowing recovery (33-35). To evaluate the potential
294 of hs-PAbW-20 gel in reducing bacterial load and improving wound repair in a diabetic model,
295 we used C57BL/6 mice. This strain was selected because it is less susceptible to
296 hyperglycaemia-induced damage compared to Balb/c mice (36). Type I diabetes was
297 chemically induced following an established protocol, and one week later, diabetic mice were
298 screened for further experimentation (**Figure S7A**) (26).

299 Consistent with earlier experiments, skin wounds were infected with *P. aeruginosa* and treated
300 on alternate days with either hs-PAbW-20 gel, control gel, or standard antibiotics. By day 7
301 post-infection, wounds treated with hs-PAbW-20 gel showed a significantly greater reduction
302 in diameter relative to day 0 compared to control gel groups (**Figure 5A–B**). Furthermore,
303 bacterial burden in internal organs was markedly lower in hs-PAbW-20–treated mice than in
304 both control and antibiotic groups (**Figure 5C**). Analysis of wound-healing markers also
305 revealed strong upregulation in the hs-PAbW-20 gel group compared with controls and
306 antibiotics (**Figure S7B–E**).

307 Improved healing with hs-PAbW-20 gel treatment was further demonstrated through tissue
308 histopathology. Wound tissue treated with the control gel still displayed necrotic epidermis,
309 inadequate re-epithelialization, and persistent inflammatory infiltrates up to day 9 (Score: 4).

310 Similarly, the antibiotic-treated groups also showed extensive inflammatory cell infiltrates
311 along with disrupted tissue architecture (Score: 4). In contrast, histopathological images of
312 wounds treated with hs-PAbW-20 gel revealed clear signs of healing, including restoration of
313 the epithelial layer, visible keratinization, varying levels of re-epithelialization, angiogenesis,
314 and even the emergence of hair follicles (Score: 2) (**Figure 6**).

315 Collectively, these findings indicate that hs-PAbW-20 gel is effective for managing infected
316 diabetic wounds and improving delayed healing.

317

318

319 Discussion

320 The skin plays a fundamental role as a barrier against environmental insults, yet its integrity
321 can be compromised by trauma, burns, ulcers, and other injuries (37-39). Wound healing is a
322 dynamic process involving haemostasis, inflammation resolution, cellular proliferation, and
323 tissue remodelling (40-42). However, microbial colonization in acute and chronic wounds often
324 disrupts this process and can result in SSIs, which are associated with higher morbidity,
325 mortality, and economic burden due to extended hospitalisation (1, 43). While local
326 antibacterial dressings are commonly applied, the rise of antimicrobial resistance has
327 significantly reduced their efficacy (44, 45). Consequently, recent research has shifted towards
328 advanced materials such as hydrogels incorporating polymeric matrices for controlled delivery
329 of antibacterial compounds to promote wound repair (46, 47).

330 In this study, we investigated a neutral pH buffered plasma-activated water gel (hs-PAbW-20
331 gel) as an alternative to antibiotic-based wound therapies. PAW is generated by exposing water
332 to air plasma and contains diverse ROS and RNS such as NO, NO_2^-, NO_3^-, O_3, ·OH, H_2O_2, and

333 O_2^-, with both short- and long-lived species contributing to its biological activity (12, 48-50).
334 Due to this unique composition, PAW displays potent antibacterial and antiviral activity and
335 has found utility in biomedical and other sectors (19, 48, 51, 52). Unlike previous work
336 emphasising acidic PAW formulations, our group developed a high-strength, neutral pH variant
337 (hs-PAbW), which retains antibacterial efficacy. Prior studies from our laboratory
338 demonstrated that hs-PAbW acts primarily through RNS-mediated mechanisms, including
339 peroxynitrite formation and nitrotyrosine generation, and that a 20% concentration (hs-PAbW-
340 20) is effective against *S. aureus* without cytotoxic effects on L929 cells (17-20).

341 To translate this into a practical wound healing strategy, we incorporated hs-PAbW-20 into a
342 gel using an edible-grade solidifying agent. The resulting formulation preserved its bactericidal
343 action and did not interfere with cell migration *in vitro*. Importantly, *in vivo* application on *P.*
344 *aeruginosa*-infected wounds in Balb/c and C57BL/6 mice significantly reduced bacterial
345 burden compared to PBS or control gel, with treatment every alternate day from day 0 to day
346 7. This reduction correlated with increased expression of wound healing markers like *Egfr* and
347 *Mmp3*. EGFR is well recognised for promoting proliferation, migration, epithelialisation, and
348 angiogenesis, which likely contributed to the faster wound closure observed in Balb/c unlike
349 C57BL/6 mice, where a Th1-driven proinflammatory response may impede healing (32, 53-
350 56). Comparison with standard topical antibiotics showed that hs-PAbW-20 gel performed on
351 par with neomycin and soframycin in reducing bacterial load and accelerating wound closure.
352 Its efficacy also extended to *S. aureus*, with reductions comparable to neomycin.

353 Given the additional complications of diabetic wounds, where hyperglycaemia leads to
354 persistent inflammation, oxidative stress, impaired angiogenesis, and heightened infection risk,
355 we evaluated hs-PAbW-20 gel in diabetic models (35, 57-59). The gel significantly lowered *P.*
356 *aeruginosa* burden in diabetic wounds, outperformed neomycin and soframycin, improved

wound healing gene expression, and reduced pathology scores. These findings highlight the potential of hs-PAbW-20 gel as a therapeutic option for chronic and diabetic wounds.

To our knowledge, this is the first report demonstrating the generation and *in vivo* application of a neutral pH plasma-activated water hydrogel. The promising results from this study suggest that hs-PAbW-20 gel may represent a new class of wound healing therapeutics with potential to address limitations of current antibiotic-based treatments.

Author contribution

Conceptualization: DM, PG, LNR, and DC, Methodology: DM, PG, RSR, KV, AG, Investigation: DM, PG, RSR, KV, AG, Visualization: DM, PG , Data curation: DM, PG, KV, AG, Formal analysis: DM, PG, KV, AG, Fund acquisition: LNR and DC, Project administration: DM, PG, KV, LNR, and DC, Writing-original draft: DM, PG, Editing and proofreading: DM, PG, LNR, and DC, Supervision: LNR and DC.

Acknowledgments

The authors gratefully acknowledge the support of the Central Flow Cytometry Facility at IISc. Special thanks are extended to Mrs. Dharani and Mr. Munish for their assistance in FACS data acquisition.

Funding

This research was supported by the DAE SRC Fellowship (DAE00195) and the DBT–IISc Partnership Umbrella Program for Advanced Research in Biological Sciences and

Bioengineering. Additional technical support from ICMR (Centre for Advanced Study in Molecular Medicine), DST (FIST), and UGC (Special Assistance) is gratefully acknowledged. DC acknowledges funding from the ASTRA Chair Professorship Grant at IISc and the TATA Innovation Fellowship. LNR thanks the Indian Institute of Science (IISc), the Biotechnology Industry Research Assistance Council, the Scheme for Transformational and Advanced Research in Sciences (STARS), and the BIRC Research Grant for financial support. DM acknowledges the IISc Fellowship provided by MHRD, Government of India. PG is grateful for the DBT–JRF Fellowship, while KV acknowledges support from the CSIR–SRA Fellowship.

Transparency statement

None to declare.

Data availability

Authors approve data availability.

Figures:

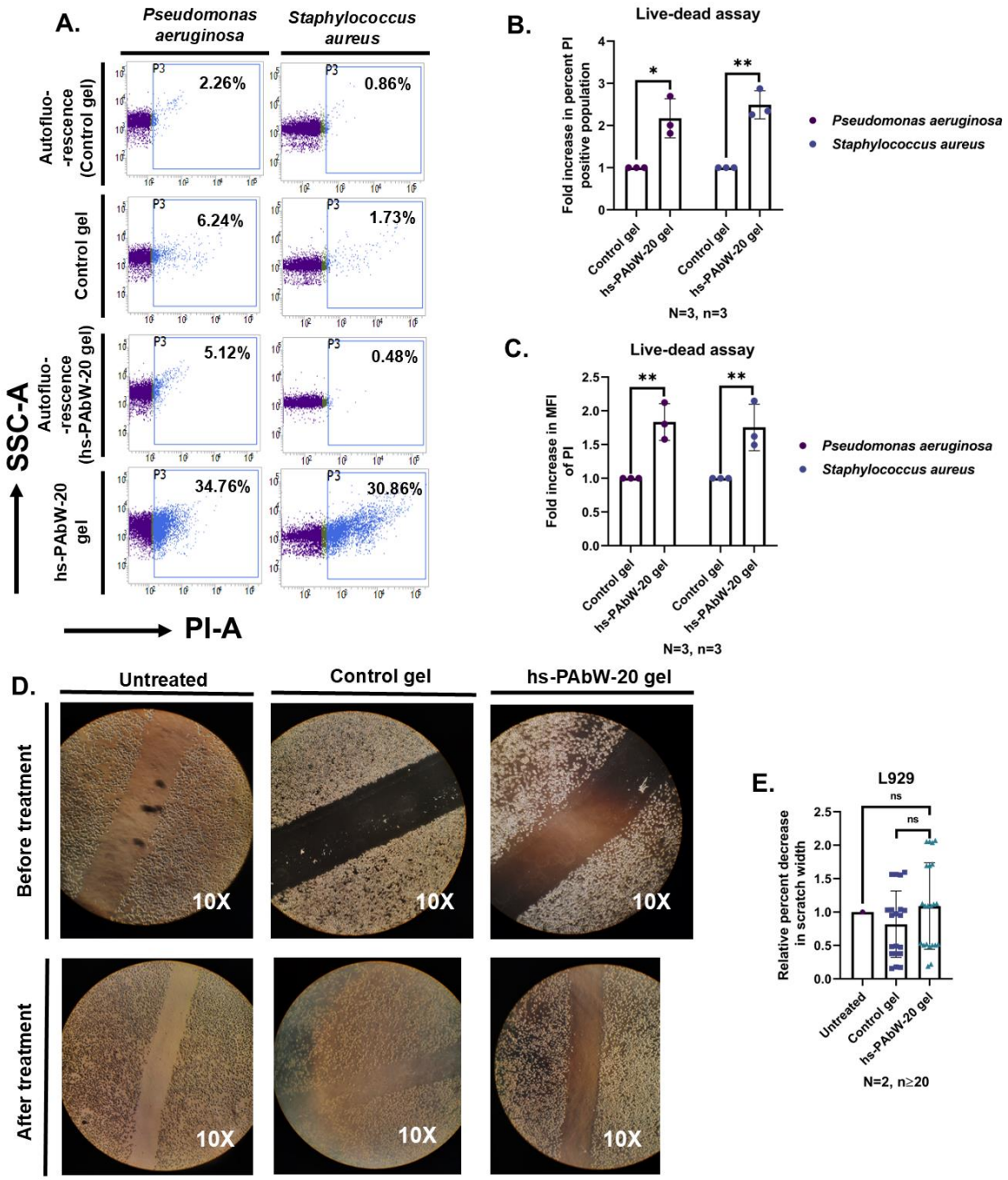

Figure 1

Figure 1: The hs-PAbW-20 gel retained its antibacterial activity without negatively influencing the migration of mouse fibroblast cells.

A. Representative dot plots (SSC-A vs. PI-A) of propidium iodide staining following treatment of *P. aeruginosa* and *S. aureus* with hs-PAbW-20 gel. Data shown are representative of N=3, n=3.

402 B. Bar graphs illustrating the fold increase in the percentage of PI-positive populations in
403 *P. aeruginosa* and *S. aureus* after treatment with hs-PAbW-20 gel. Values are presented
404 as mean ± SD, representative of N=3, n=3.
405 C. Bar graphs depicting the fold increase in PI MFI upon exposure of *P. aeruginosa* and
406 *S. aureus* to hs-PAbW-20 gel. Data are presented as mean ± SD, representative of N=3,
407 n=3.
408 D. Representative images of L929 cell scratch assays before (0 h) and after (24 h) hs-
409 PAbW-20 gel treatment. Images are representative of N=2, n ≥ 20.
410 E. Bar graphs showing the relative percentage decrease in L929 scratch width following
411 24 h exposure to hs-PAbW-20 gel. Data are presented as mean ± SD, representative of
412 N=2, n ≥ 20.

413 (One-way ANOVA for column graphs and line graphs, Two-way ANOVA for grouped data,
414 Mann-Whitney U-test for animal CFU data (**** $p < 0.0001$, *** $p < 0.001$, ** $p<0.01$, *
415 $p<0.05$))

416

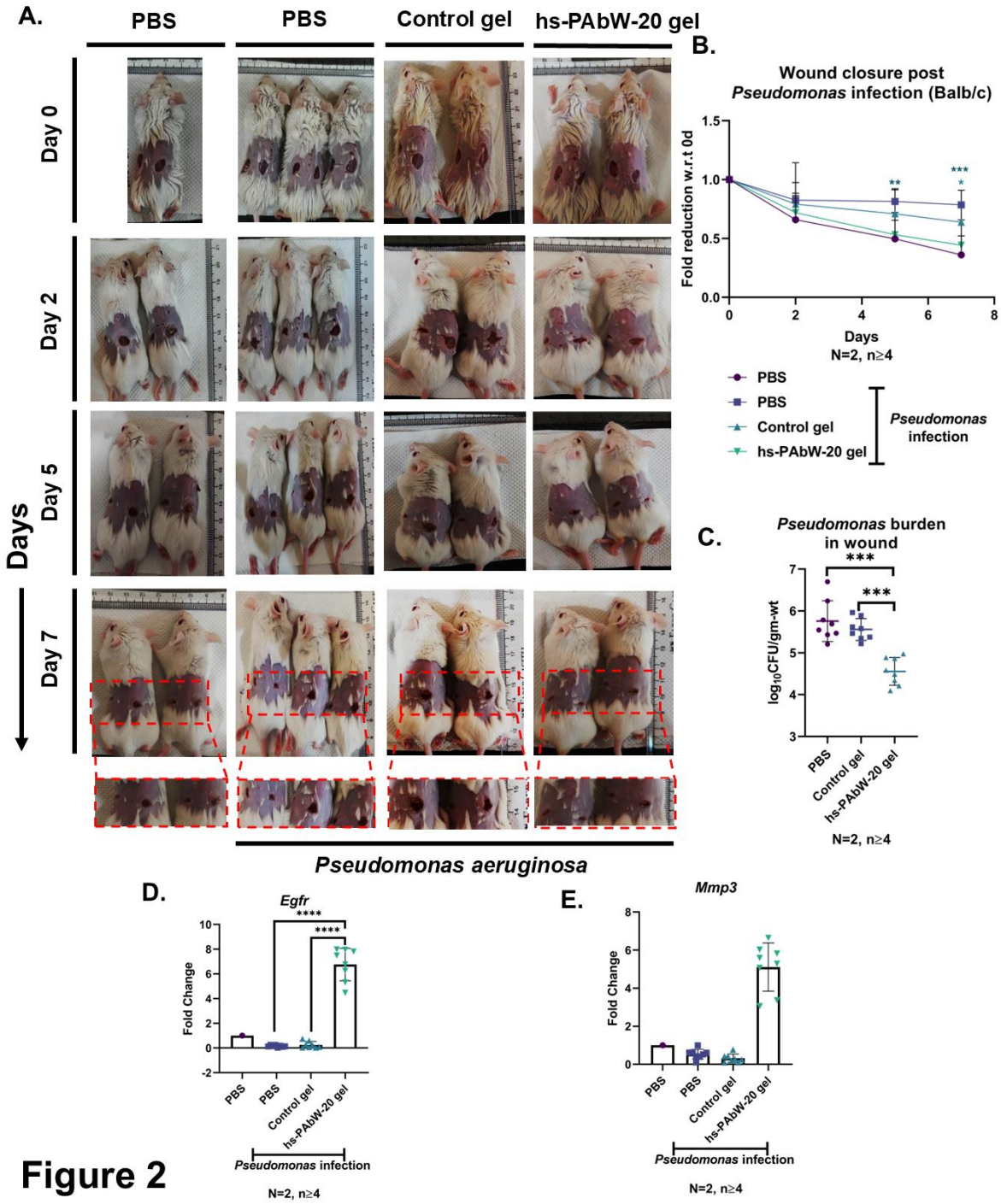

Figure 2

Figure 2: Treatment with hs-PAbW-20 gel resulted in decreased *P. aeruginosa* load in infected wounds, accelerated wound closure, and increased transcriptional expression of genes associated with wound healing.

A. Representative images of wounds in Balb/c mice following *P. aeruginosa* infection (Day 0) and subsequent treatment with PBS, control gel, or hs-PAbW-20 gel, captured on alternate days up to day 7. Data shown are from N=2, n≥4.

B. Line graphs illustrating the fold reduction in wound diameter relative to day 0, with or without *P. aeruginosa* infection, and treatment using PBS, control gel, or hs-PAbW-20 gel. Data combined from N=2, n≥4 and presented as mean ± SD.

C. Bacterial load of *P. aeruginosa* in wounds after treatment with 1X PBS, control gel, or hs-PAbW-20 gel. Data pooled from N=2, n≥4 and presented as mean ± SD.

D. Gene expression levels of *Egfr* in uninfected samples and in infected samples treated with PBS, control gel, or hs-PAbW-20 gel. Data shown as mean ± SD, representative of N=2, n≥4.

E. Gene expression levels of *Mmp3* in uninfected samples and in infected samples treated with PBS, control gel, or hs-PAbW-20 gel. Data shown as mean ± SD, representative of N=2, n≥4.

(One-way ANOVA for column graphs and line graphs, Two-way ANOVA for grouped data, Mann-Whitney U-test for animal CFU data (**** $p < 0.0001$, *** $p < 0.001$, ** $p<0.01$, * $p<0.05$))

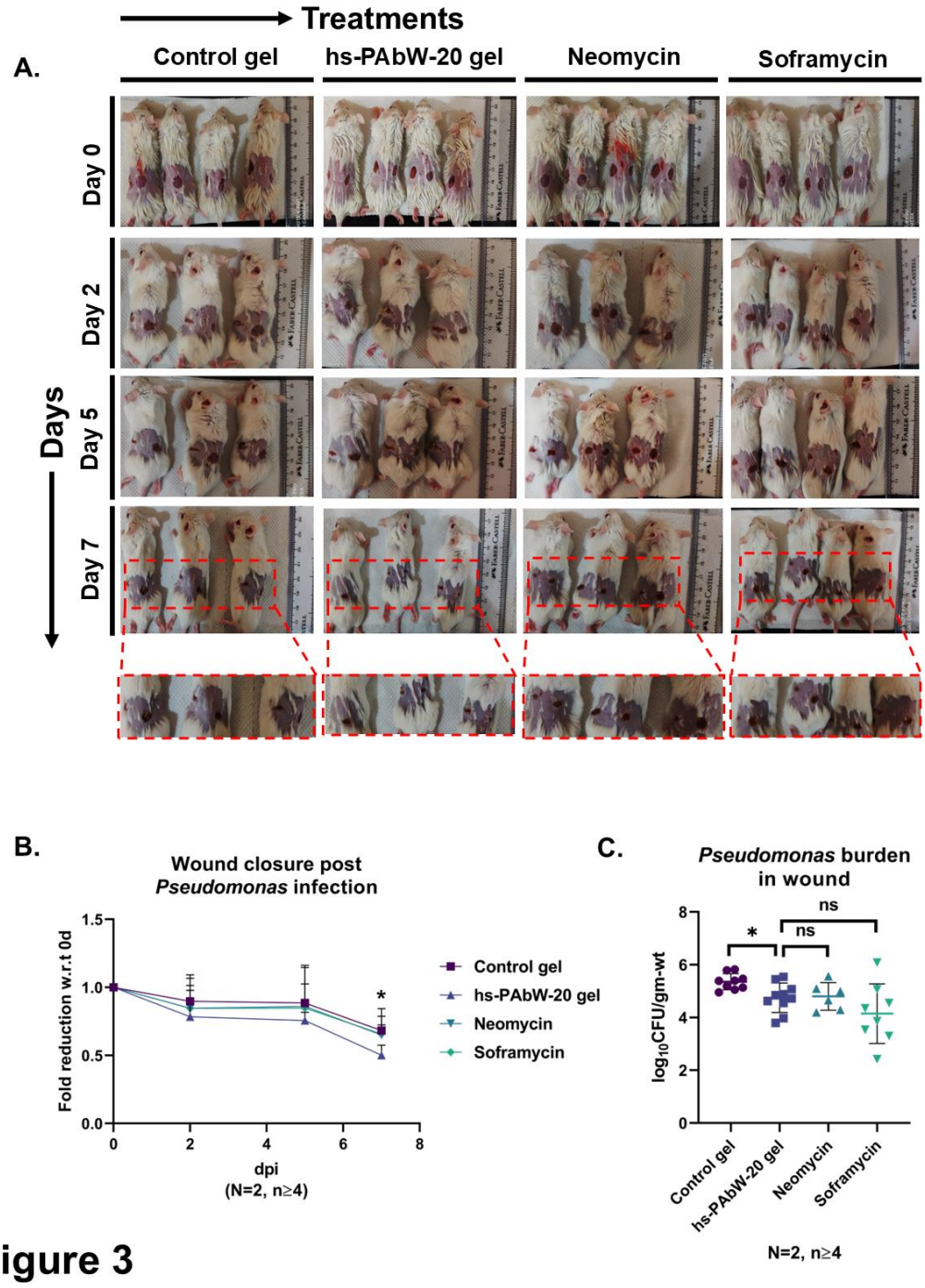

Figure 3

439

440

441 **Figure 3: The hs-PAbW-20 gel showed effectiveness similar to that of standard antibiotic**

442 **creams in lowering *P. aeruginosa* burden in wounds within the *in vivo* model.**

A. Representative images of wounds in Balb/c mice post *P. aeruginosa* infection (Day 0) and subsequent treatment with control gel, hs-PAbW-20 gel, neomycin, or soframycin, documented on alternate days through day 7. Data shown are from N=2, n≥4.

B. Line graphs depicting the fold reduction in wound diameter compared to day 0 following *P. aeruginosa* infection and treatment with control gel, hs-PAbW-20 gel, neomycin, or soframycin. Data combined from N=2, n≥4 and presented as mean ± SD.

C. Quantification of *P. aeruginosa* burden in wounds after treatment with control gel, hs-PAbW-20 gel, neomycin, or soframycin. Data pooled from N=2, n≥4 and presented as mean ± SD.

(One-way ANOVA for column graphs and line graphs, Two-way ANOVA for grouped data, Mann-Whitney U-test for animal CFU data (**** $p < 0.0001$, *** $p < 0.001$, ** $p<0.01$, * $p<0.05$))

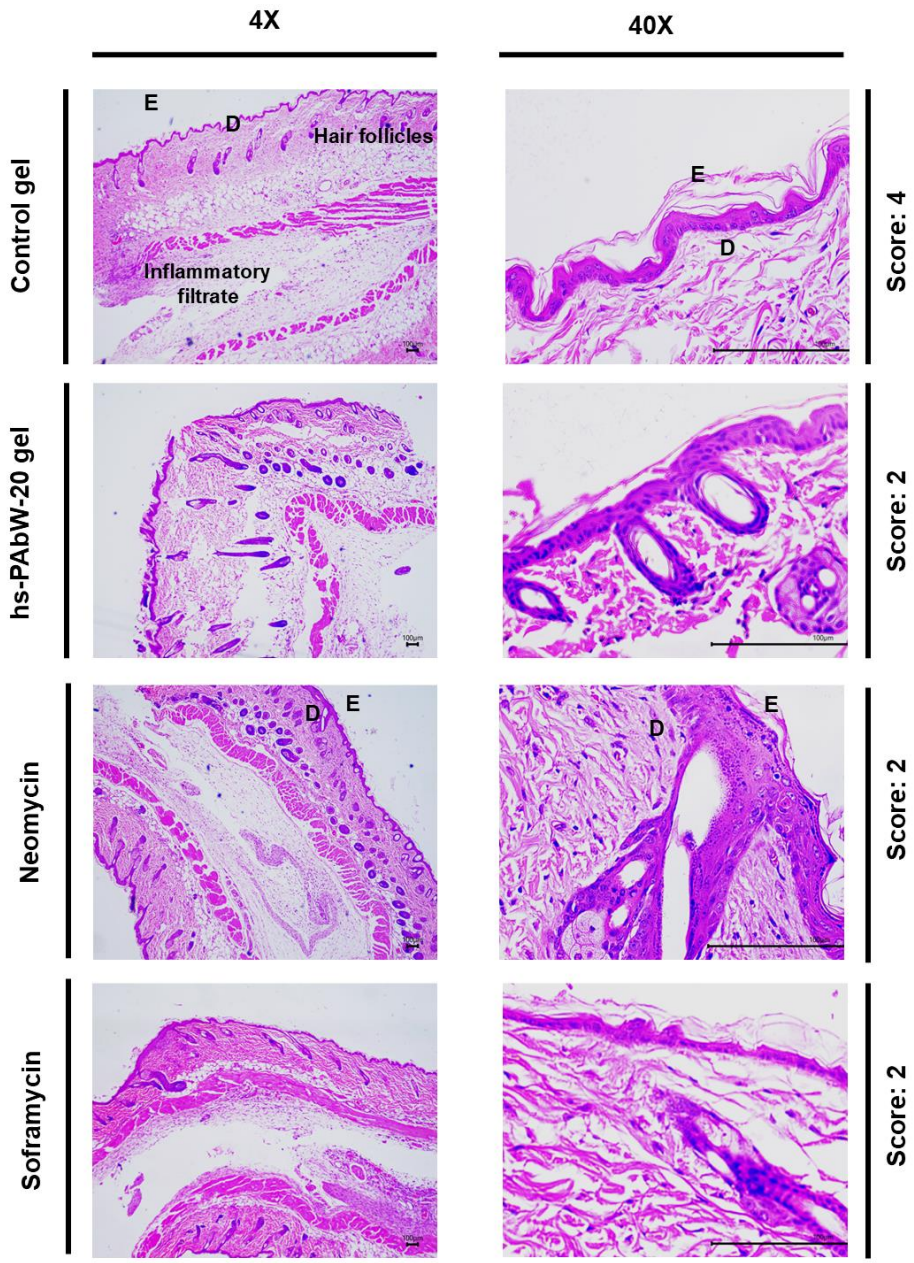

Scoring system: The scoring of the pathological changes are graded as 0-4; for each of the pathological lesions (Severe/ marked -4 ; Moderate -3; mild -2; Minor/minimum -1; No pathology -0) considering the following pathological lesions, inflammation and edema.

456 **Figure 4**

457 **Figure 4. Histopathological analysis demonstrates enhanced healing of *P. aeruginosa*-**
458 **infected wounds treated with hs-PAbW-20 gel compared to control gel, with outcomes**
459 **comparable to those observed with neomycin and soframycin.**

460 Haematoxylin and eosin–stained sections depict wound pathology following treatment with
461 control gel, hs-PAbW-20 gel, neomycin, or soframycin.

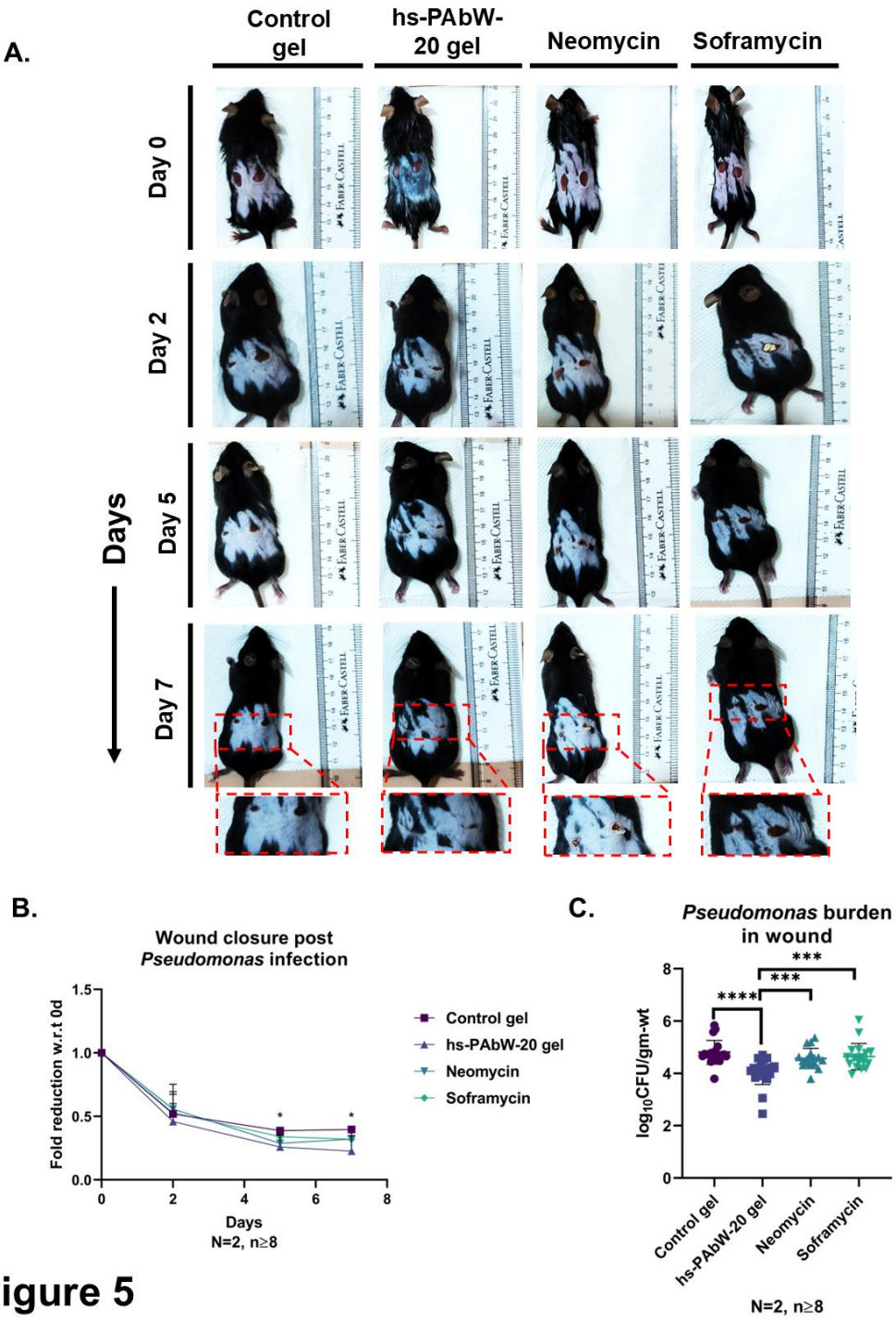

Figure 5

Figure 5: The hs-PAbW-20 gel significantly lowers bacterial load in *P. aeruginosa*–infected wounds of diabetic mice and promotes enhanced wound closure.

A. Representative images of wounds in diabetic C57BL/6 mice following *P. aeruginosa* infection (Day 0) and treatment with control gel, hs-PAbW-20 gel, neomycin, or soframycin, recorded on alternate days up to day 7. Data shown are from N=2, n≥8.

468 B. Line graphs showing the fold reduction in wound diameter of diabetic mice relative to
469 day 0 after *P. aeruginosa* infection and treatment with control gel, hs-PAbW-20 gel,
470 neomycin, or soframycin. Data combined from N=2, n≥8 and presented as mean ±
471 SD.
472 C. Bacterial load of *P. aeruginosa* in wounds of diabetic mice following treatment with
473 control gel, hs-PAbW-20 gel, neomycin, or soframycin. Data pooled from N=2, n≥8
474 and presented as mean ± SD.

475 (One-way ANOVA for column graphs and line graphs, Two-way ANOVA for grouped data,
476 Mann-Whitney U-test for animal CFU data (**** $p < 0.0001$, *** $p < 0.001$, ** $p<0.01$, *
477 $p<0.05$))

478

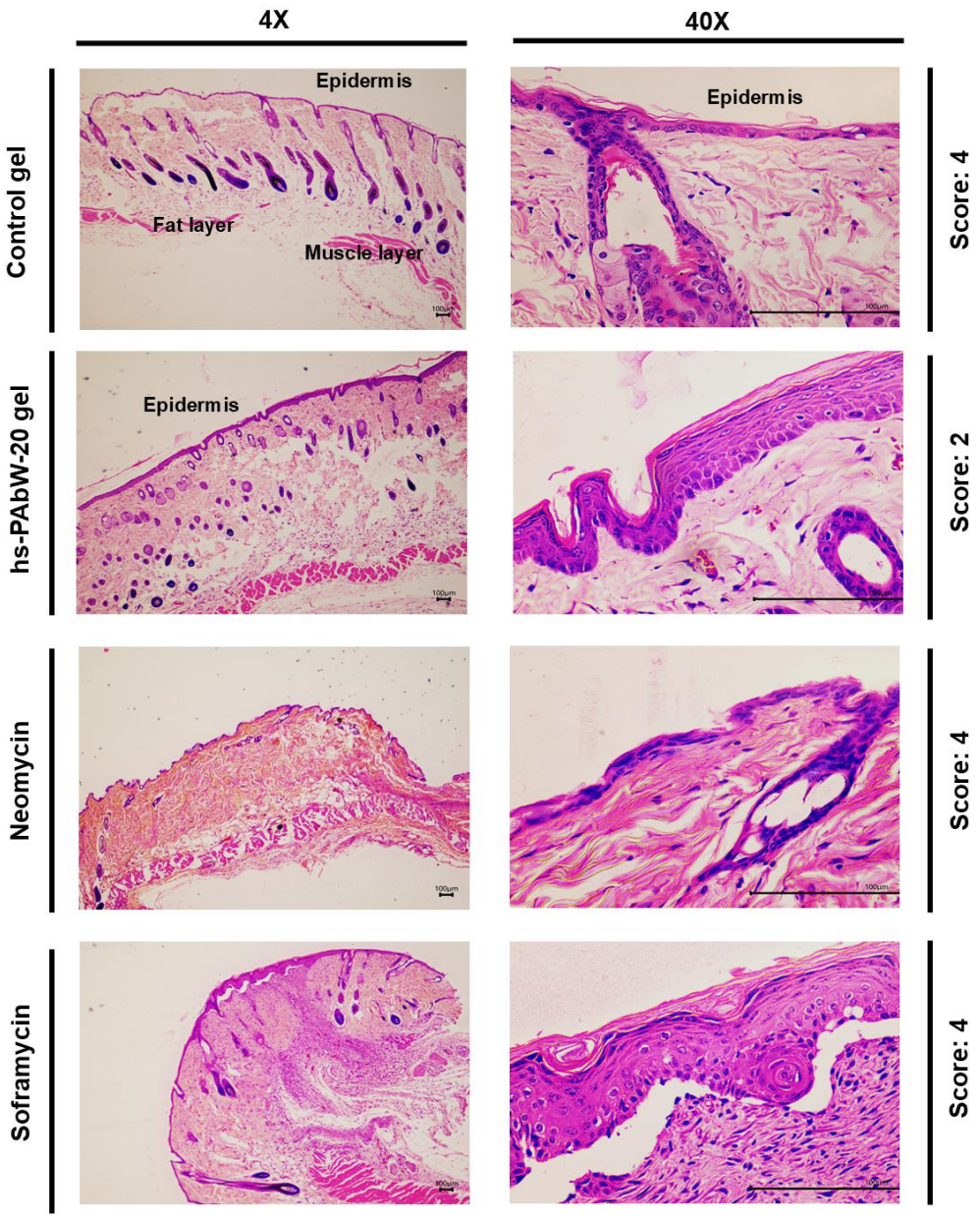

Scoring system: The scoring of the pathological changes are graded as 0-4; for each of the pathological lesions (Severe/ marked -4 ; Moderate -3; mild -2; Minor/minimum -1; No pathology -0) considering the following pathological lesions, inflammation, edema, re-epithelialization and necrosed epidermis

Figure 6

Figure 6: Histopathological analysis confirms enhanced wound closure in diabetic mice treated with hs-PAbW-20 gel.

Haematoxylin and eosin–stained sections illustrate wound pathology after treatment with control gel, hs-PAbW-20 gel, neomycin, or soframycin.

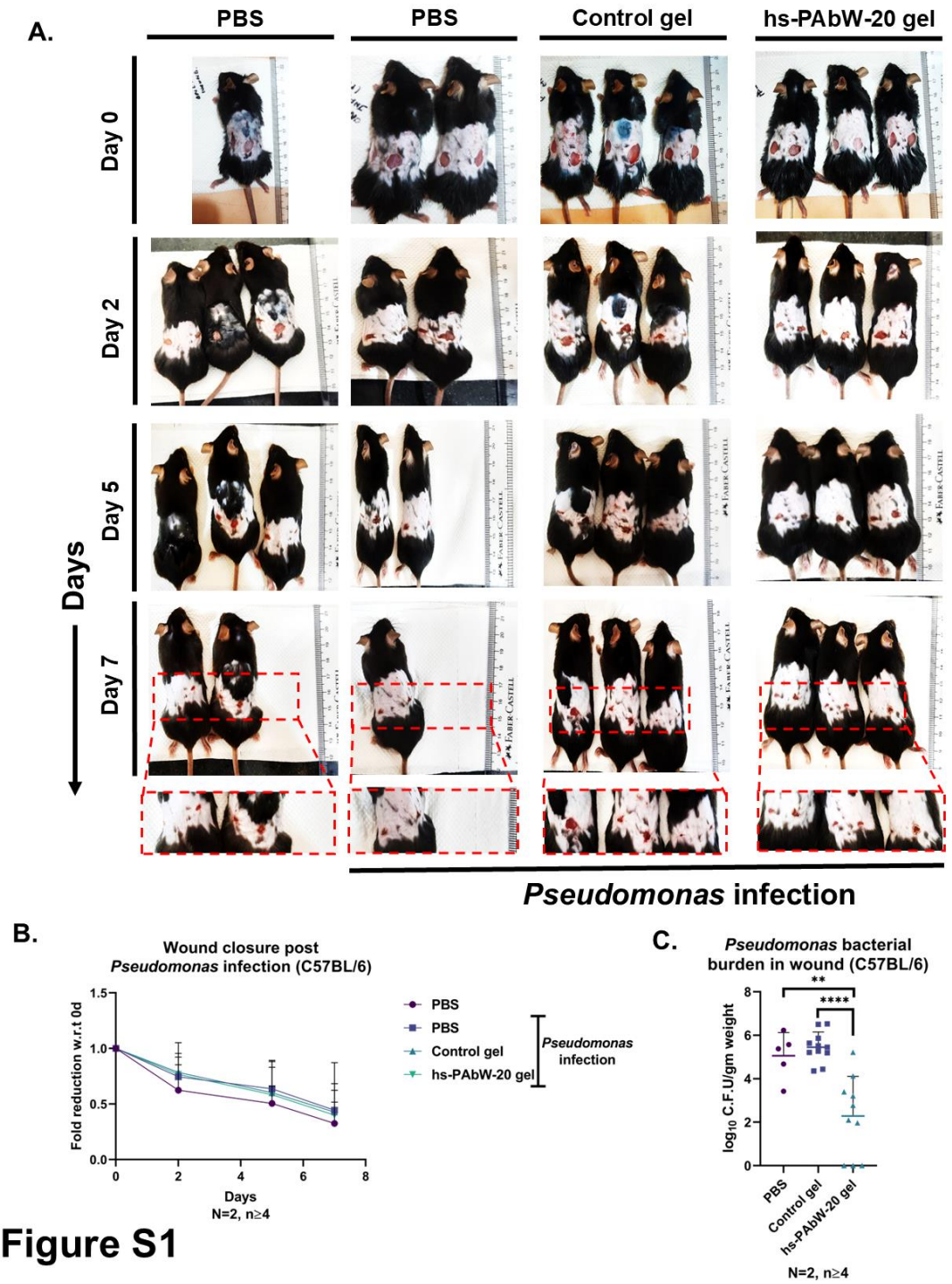

Figure S1. hs-PAbW-20 gel reduced the bacterial load in *P. aeruginosa*–infected wounds of C57BL/6 mice but did not significantly affect wound closure.

A. Representative images of wounds in C57BL/6 mice post *P. aeruginosa* infection (Day 0) and treatment with PBS, control gel, or hs-PAbW-20 gel, recorded on alternate days through day 7. Data shown are from N=2, n≥4.

B. Line graphs showing fold reduction in wound diameter of C57BL/6 mice relative to day 0, with or without *P. aeruginosa* infection, following treatment with PBS, control gel, or hs-PAbW-20 gel. Data combined from N=2, n≥4 and presented as mean ± SD.

C. Quantification of *P. aeruginosa* burden in wounds of C57BL/6 mice treated with 1X PBS, control gel, or hs-PAbW-20 gel. Data pooled from N=2, n≥4 and presented as mean ± SD.

(One-way ANOVA for column graphs and line graphs, Two-way ANOVA for grouped data, Mann-Whitney U-test for animal CFU data (**** $p < 0.0001$, *** $p < 0.001$, ** $p<0.01$, * $p<0.05$))

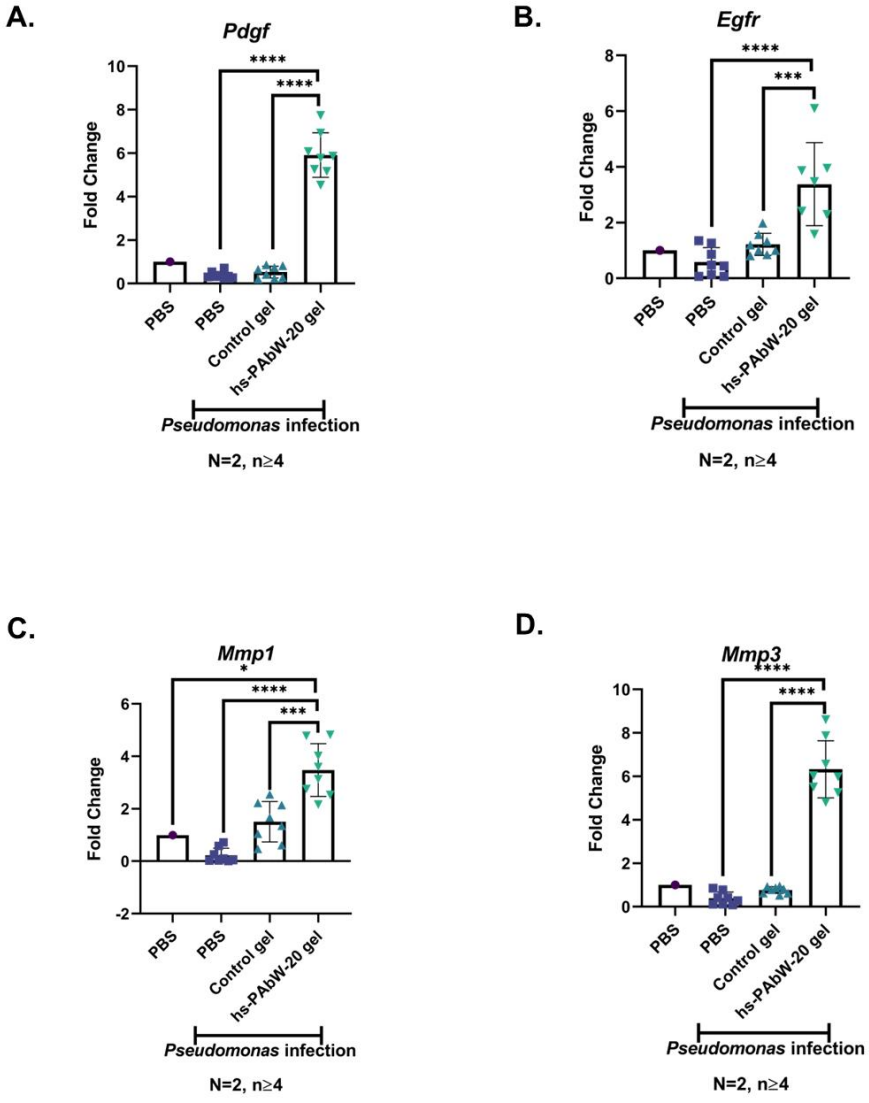

Figure S2

Figure S2. hs-PAbW-20 gel enhanced the transcriptional expression of wound-healing markers in C57BL/6 mouse wounds.

A. Expression of *Pdgf* in uninfected wounds and in infected wounds treated with PBS, control gel, or hs-PAbW-20 gel. Data shown as mean ± SD, representative of N=2, n≥4.

B. Expression of *Egfr* in uninfected wounds and in infected wounds treated with PBS, control gel, or hs-PAbW-20 gel. Data shown as mean ± SD, representative of N=2, n≥4.

C. Expression of *Mmp1* in uninfected wounds and in infected wounds treated with PBS, control gel, or hs-PAbW-20 gel. Data shown as mean ± SD, representative of N=2, n≥4.

D. Expression of *Mmp3* in uninfected wounds and in infected wounds treated with PBS, control gel, or hs-PAbW-20 gel. Data shown as mean ± SD, representative of N=2, n≥4.

(One-way ANOVA for column graphs and line graphs, Two-way ANOVA for grouped data, Mann-Whitney U-test for animal CFU data (**** $p < 0.0001$, *** $p < 0.001$, ** $p<0.01$, * $p<0.05$))

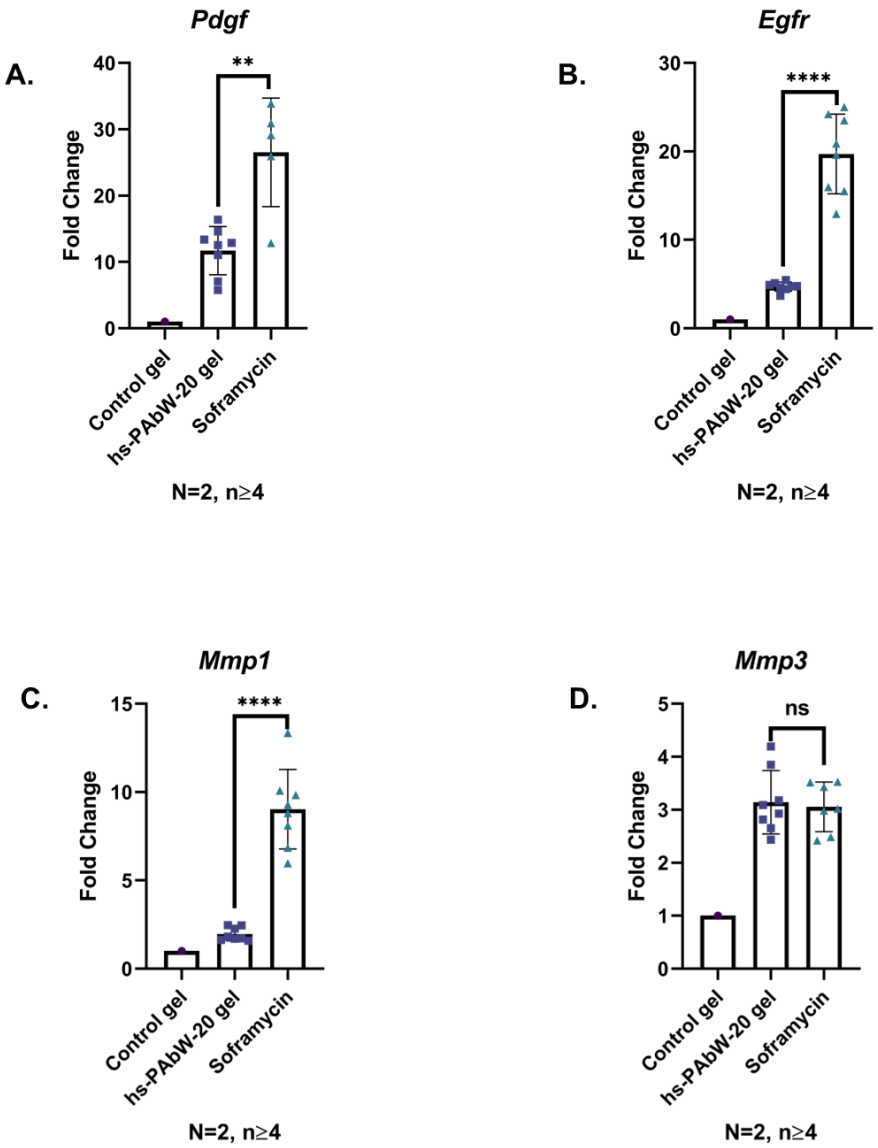

Figure S3

Figure S3: hs-PAbW-20 gel enhanced the transcriptional expression of wound-healing markers in Balb/c mouse wounds, in same line as soframycin antibiotic.

522 A. Levels of *Pdgf* expression in *P. aeruginosa*-infected wounds of Balb/c mice following
523 treatment with control gel, hs-PAbW-20 gel, or soframycin. Data shown as mean ± SD,
524 representative of N=2, n≥4.
525 B. Levels of *Egfr* expression in *P. aeruginosa*-infected wounds of Balb/c mice after
526 treatment with control gel, hs-PAbW-20 gel, or soframycin. Data shown as mean ± SD,
527 representative of N=2, n≥4.
528 C. Levels of *Mmp1* expression in *P. aeruginosa*-infected wounds of Balb/c mice post-
529 treatment with control gel, hs-PAbW-20 gel, or soframycin. Data shown as mean ± SD,
530 representative of N=2, n≥4.
531 D. Levels of *Mmp3* expression in *P. aeruginosa*-infected wounds of Balb/c mice following
532 treatment with control gel, hs-PAbW-20 gel, or soframycin. Data shown as mean ± SD,
533 representative of N=2, n≥4.

534 (One-way ANOVA for column graphs and line graphs, Two-way ANOVA for grouped data,
535 Mann-Whitney U-test for animal CFU data (**** $p < 0.0001$, *** $p < 0.001$, ** $p<0.01$, *
536 $p<0.05$))

537

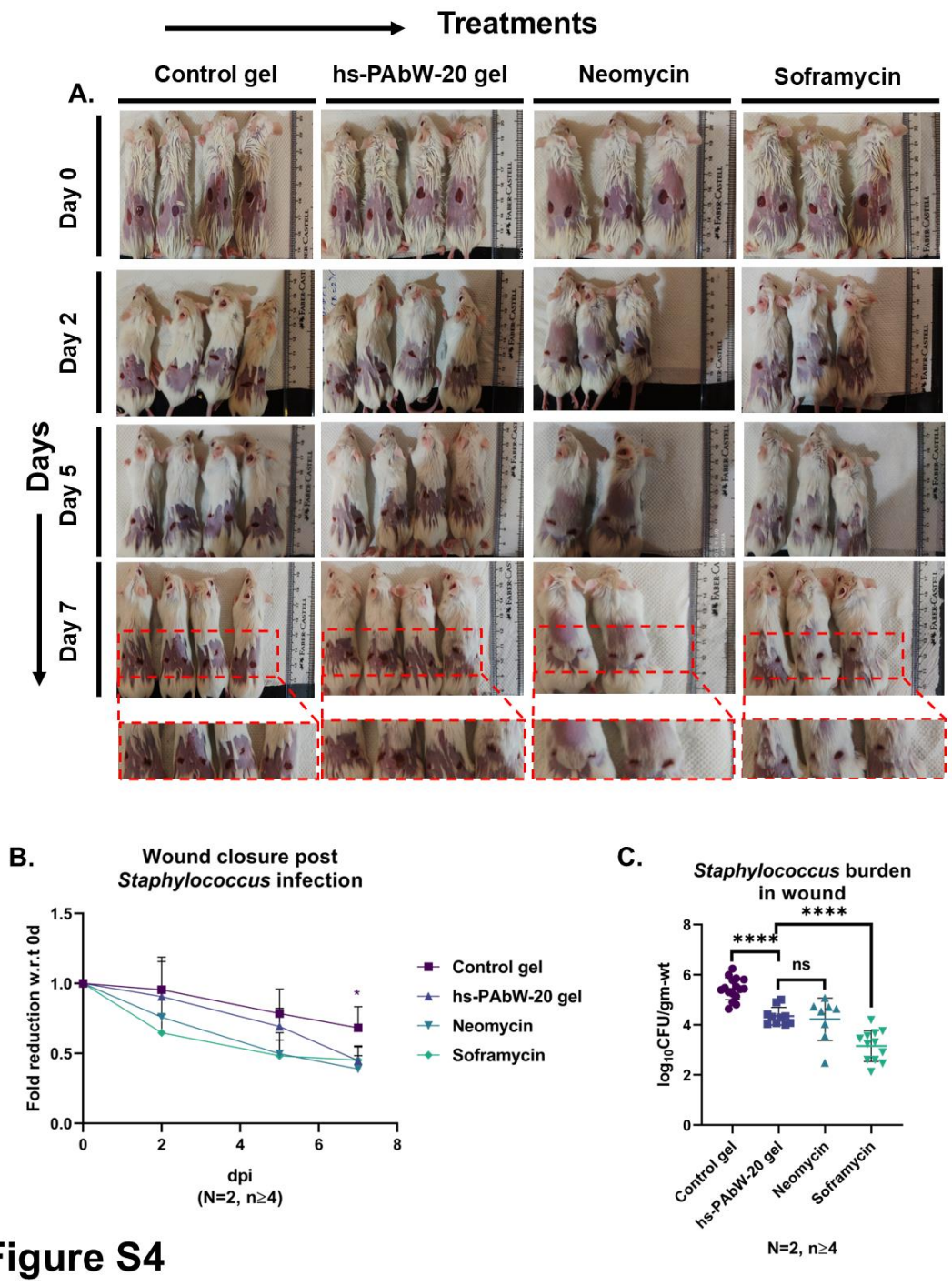

Figure S4

538

539 **Figure S4: The hs-PAbW-20 gel performed comparably to standard antibiotic creams in**

540 **reducing *S. aureus* burden in wounds within the Balb/c mouse *in vivo* model.**

541 A. Representative images of wounds in Balb/c mice following *S. aureus* infection (Day 0)
542 and treatment with control gel, hs-PAbW-20 gel, neomycin, or soframycin, recorded
543 every other day up to day 7. Data shown are from N=2, n≥4.
544 B. Line graphs illustrating the fold reduction in wound diameter relative to day 0 after *S.*
545 *aureus* infection and treatment with control gel, hs-PAbW-20 gel, neomycin, or
546 soframycin. Data combined from N=2, n≥4 and presented as mean ± SD.
547 C. Quantification of *S. aureus* burden in wounds post-treatment with control gel, hs-
548 PAbW-20 gel, neomycin, or soframycin. Data pooled from N=2, n≥4 and presented as
549 mean ± SD.

550 (One-way ANOVA for column graphs and line graphs, Two-way ANOVA for grouped data,
551 Mann-Whitney U-test for animal CFU data (**** $p < 0.0001$, *** $p < 0.001$, ** $p<0.01$, *
552 $p<0.05$))

553

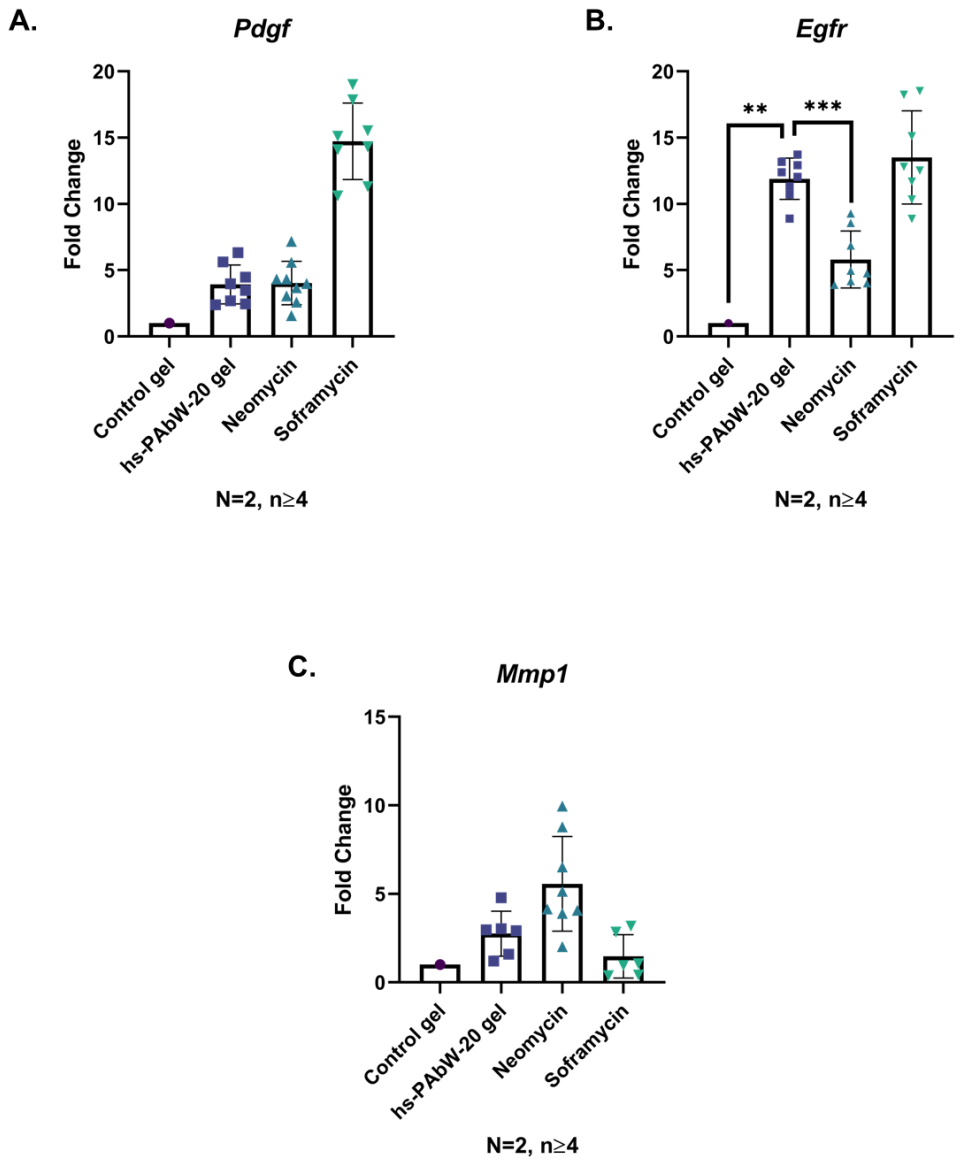

Figure S5

554

555 **Figure S5: hs-PAbW-20 gel enhanced the transcriptional expression of wound-healing**

556 **markers in Balb/c mice wounds, infected with *S. aureus*.**

557 A. Expression levels of *Pdgf* in *S. aureus*-infected wounds of Balb/c mice treated with
558 control gel, hs-PAbW-20 gel, neomycin, or soframycin. Data shown as mean ± SD,
559 representative of N=2, n≥4.
560 B. Expression levels of *Egfr* in *S. aureus*-infected wounds of Balb/c mice following
561 treatment with control gel, hs-PAbW-20 gel, neomycin, or soframycin. Data shown as
562 mean ± SD, representative of N=2, n≥4.
563 C. Expression levels of *Mmp1* in *S. aureus*-infected wounds of Balb/c mice after treatment
564 with control gel, hs-PAbW-20 gel, neomycin, or soframycin. Data shown as mean ±
565 SD, representative of N=2, n≥4.

566 (One-way ANOVA for column graphs and line graphs, Two-way ANOVA for grouped data,
567 Mann-Whitney U-test for animal CFU data (**** $p < 0.0001$, *** $p < 0.001$, ** $p<0.01$, *
568 $p<0.05$))

569

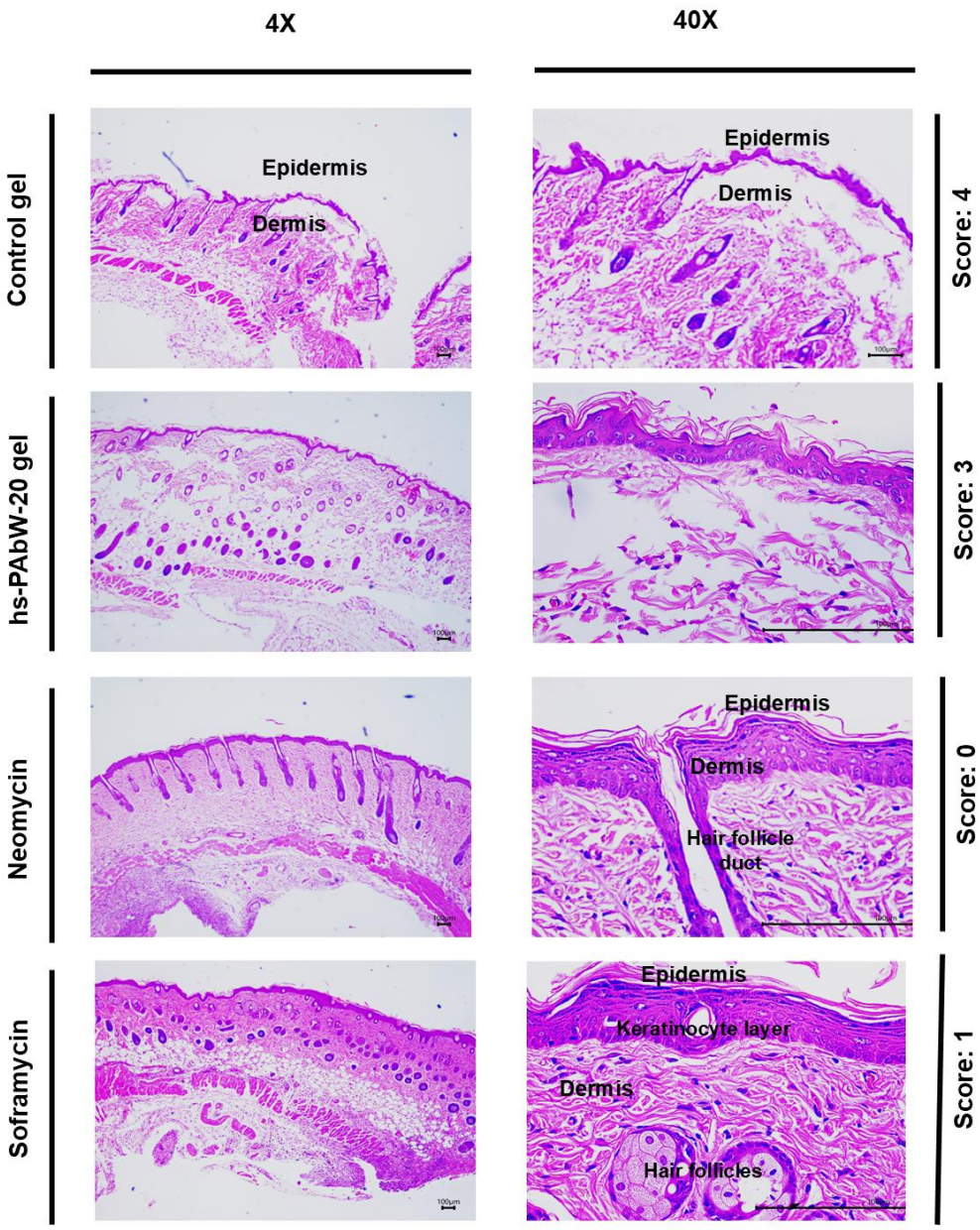

Scoring system: The scoring of the pathological changes are graded as 0-4; for each of the pathological lesions (Severe/ marked -4 ; Moderate -3; mild -2; Minor/minimum -1; No pathology -0) considering the following pathological lesions, inflammation and edema.

Figure S6

570

571 **Figure S6: Histopathological analysis reveals improved healing of *S. aureus*-infected**

572 **wounds compared to the control gel.**

573 Haematoxylin and eosin–stained sections depict the pathology of *S. aureus*-infected wounds

574 following treatment with control gel, hs-PAbW-20 gel, neomycin, or soframycin.

575

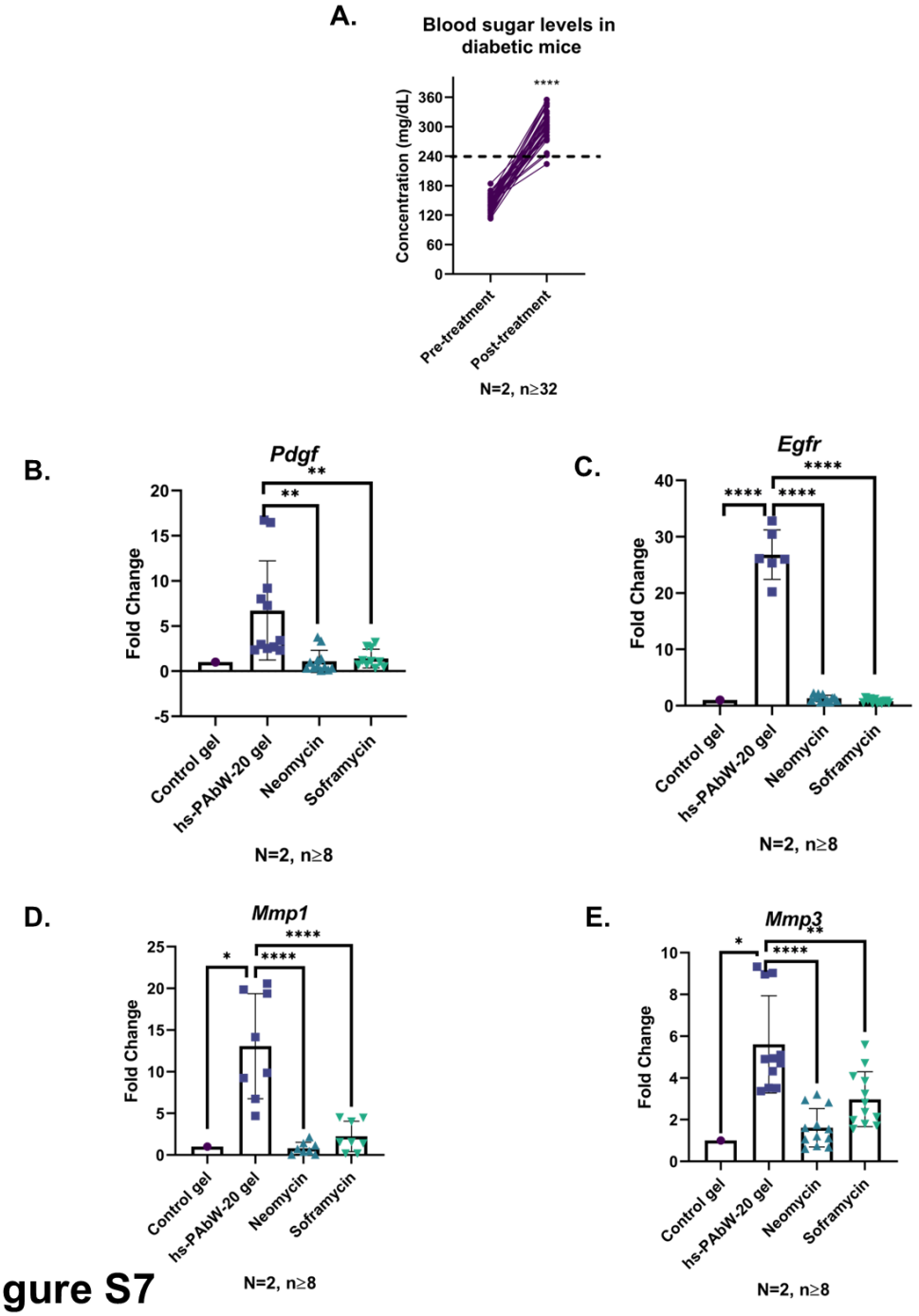

Figure S7

576

577 **Figure S7: The hs-PAbW-20 gel promoted increased transcriptional expression of wound-**

578 **healing markers in *P. aeruginosa*-infected wounds of diabetic C57BL/6 mice.**

A. Blood glucose levels in C57BL/6 mice before and after streptozotocin treatment. Data representative of N=2, n≥32 and is presented as mean ± SD.

B. Expression levels of *Pdgf* in *P. aeruginosa*-infected wounds of diabetic C57BL/6 mice treated with control gel, hs-PAbW-20 gel, neomycin, or soframycin. Data shown as mean ± SD, representative of N=2, n≥8.

C. Expression levels of *Egfr* in *P. aeruginosa*-infected wounds of diabetic C57BL/6 mice following treatment with control gel, hs-PAbW-20 gel, neomycin, or soframycin. Data shown as mean ± SD, representative of N=2, n≥8.

D. Expression levels of *Mmp1* in *P. aeruginosa*-infected wounds of diabetic C57BL/6 mice post-treatment with control gel, hs-PAbW-20 gel, neomycin, or soframycin. Data shown as mean ± SD, representative of N=2, n≥8.

E. Expression levels of *Mmp3* in *P. aeruginosa*-infected wounds of diabetic C57BL/6 mice treated with control gel, hs-PAbW-20 gel, neomycin, or soframycin. Data shown as mean ± SD, representative of N=2, n≥8.

(One-way ANOVA for column graphs and line graphs, Two-way ANOVA for grouped data, Mann-Whitney U-test for animal CFU data (**** $p < 0.0001$, *** $p < 0.001$, ** $p<0.01$, * $p<0.05$))

References:

1. Arora A, Bharadwaj P, Chaturvedi H, Chowbey P, Gupta S, Leaper D, et al. A review of prevention of surgical site infections in Indian hospitals based on global guidelines for the prevention of surgical site infection, 2016. Journal of Patient Safety and Infection Control. 2018;6(1):1-12.
2. Owens CD, Stoessel K. Surgical site infections: epidemiology, microbiology and prevention. J Hosp Infect. 2008;70 Suppl 2:3-10.

3. Mangram AJ, Horan TC, Pearson ML, Silver LC, Jarvis WR, Committee HICPA. Guideline for prevention of surgical site infection, 1999. Infection Control & Hospital Epidemiology. 1999;20(4):247-80.
4. Emori TG, Gaynes RP. An overview of nosocomial infections, including the role of the microbiology laboratory. Clinical microbiology reviews. 1993;6(4):428-42.
5. Negut I, Grumezescu V, Grumezescu AM. Treatment Strategies for Infected Wounds. Molecules. 2018;23(9).
6. Taati Moghadam M, Khoshbayan A, Chegini Z, Farahani I, Shariati A. Bacteriophages, a New Therapeutic Solution for Inhibiting Multidrug-Resistant Bacteria Causing Wound Infection: Lesson from Animal Models and Clinical Trials. Drug Des Devel Ther. 2020;14:1867-83.
7. Glik J, Kawecki M, Gazdzik T, Nowak M. The impact of the types of microorganisms isolated from blood and wounds on the results of treatment in burn patients with sepsis. Pol Przegl Chir. 2012;84(1):6-16.
8. Maillard JY, Kampf G, Cooper R. Antimicrobial stewardship of antiseptics that are pertinent to wounds: the need for a united approach. JAC Antimicrob Resist. 2021;3(1):dlab027.
9. Eeshita D, Tejashree Anantharaj U, Krishna Karthik M. Antimicrobial Susceptibility Profile of Methicillin Resistant Staphylococcus Aureus (MRSA) Isolates in a Tertiary Care Hospital, Mysuru, India. Indian Journal of Public Health Research & Development. 2023;14(2):88-93.
10. Dash M, Padhi S, Narasimham M, Pattnaik S. Antimicrobial resistance pattern of Pseudomonas aeruginosa isolated from various clinical samples in a tertiary care hospital, South Odisha, India. Saudi Journal for Health Sciences. 2014;3(1):15-9.
11. Rajan A, Boopathy B, Radhakrishnan M, Rao L, Schlüter OK, Tiwari BK. Plasma processing: a sustainable technology in agri-food processing. Sustainable Food Technology. 2023;1(1):9-49.
12. Thirumdas R, Kothakota A, Annapure U, Siliveru K, Blundell R, Gatt R, et al. Plasma activated water (PAW): Chemistry, physico-chemical properties, applications in food and agriculture. Trends in Food Science & Technology. 2018;77:21-31.
13. Girard PM, Arbabian A, Fleury M, Bauville G, Puech V, Dutreix M, et al. Synergistic Effect of H2O2 and NO2 in Cell Death Induced by Cold Atmospheric He Plasma. Sci Rep. 2016;6:29098.
14. Hoeben WFLM, van Ooij PP, Schram DC, Huiskamp T, Pemen AJM, Lukeš P. On the Possibilities of Straightforward Characterization of Plasma Activated Water. Plasma Chemistry and Plasma Processing. 2019;39(3):597-626.
15. Punith N, Harsha R, Lakshminarayana R, Hemanth M, S. Anand M, Dasappa S. Plasma Activated Water Generation and its Application in Agriculture. Advanced Materials Letters. 2019;10(10):700-4.
16. Han L, Boehm D, Patil S, Cullen PJ, Bourke P. Assessing stress responses to atmospheric cold plasma exposure using Escherichia coli knock-out mutants. J Appl Microbiol. 2016;121(2):352-63.
17. N. P, Singh AK, J. A, Boopathy B, Chatterjee R, M. H, et al. Generation of neutral pH high-strength plasma-activated water from a pin to water discharge and its bactericidal activity on multidrug-resistant pathogens. Plasma Processes and Polymers. 2023;20(1):2200133.

18. Zhou R, Zhou R, Prasad K, Fang Z, Speight R, Bazaka K, et al. Cold atmospheric plasma activated water as a prospective disinfectant: the crucial role of peroxynitrite. Green Chemistry. 2018;20(23):5276-84.
19. Boopathy B, Mukherjee D, Nishanth V, Chowdhury AR, Chakravortty D, Rao L. Generation of Species-Specific High-Strength Plasma Activated Water at Neutral pH and its Antimicrobial Characteristics. Plasma Chemistry and Plasma Processing. 2024;44(2):1003-17.
20. Mukherjee D, Roy Chowdhury A, Ghosh P, Vishwa N, Rao L, Chakravortty D. Reactive nitrogen species (RNS) and its reaction intermediates with reactive oxygen species (ROS) in pH-neutral high-strength plasma-activated water determines the antimicrobial activity against ESKAPE Pathogens. bioRxiv. 2024:2024.10. 06.616848.
21. Chowdhury AR, Mukherjee D, Singh AK, Chakravortty D. Loss of outer membrane protein A (OmpA) impairs the survival of Salmonella Typhimurium by inducing membrane damage in the presence of ceftazidime and meropenem. J Antimicrob Chemother. 2022;77(12):3376-89.
22. Mukherjee D, Wagle S, Ghosh P, Biswas A, Chakravortty D. Intracellular formate is a critical mediator of the antimicrobial fate of Salmonella Typhimurium Against meropenem and ciprofloxacin. 2025.
23. Bolla SR, Mohammed Al-Subaie A, Yousuf Al-Jindan R, Papayya Balakrishna J, Kanchi Ravi P, Veeraraghavan VP, et al. In vitro wound healing potency of methanolic leaf extract of Aristolochia saccata is possibly mediated by its stimulatory effect on collagen-1 expression. Heliyon. 2019;5(5):e01648.
24. Liang CC, Park AY, Guan JL. In vitro scratch assay: a convenient and inexpensive method for analysis of cell migration in vitro. Nat Protoc. 2007;2(2):329-33.
25. Huang Y, Yang N, Teng D, Mao R, Hao Y, Ma X, et al. Antibacterial peptide NZ2114-loaded hydrogel accelerates Staphylococcus aureus-infected wound healing. Appl Microbiol Biotechnol. 2022;106(9-10):3639-56.
26. Furman BL. Streptozotocin-Induced Diabetic Models in Mice and Rats. Curr Protoc. 2021;1(4):e78.
27. Serra R, Grande R, Butrico L, Rossi A, Settimio UF, Caroleo B, et al. Chronic wound infections: the role of Pseudomonas aeruginosa and Staphylococcus aureus. Expert Rev Anti Infect Ther. 2015;13(5):605-13.
28. Alonso-Matilla R, Provenzano PP, Odde DJ. Physical principles and mechanisms of cell migration. NPJ Biol Phys Mech. 2025;2(1):2.
29. Barrientos S, Stojadinovic O, Golinko MS, Brem H, Tomic-Canic M. Growth factors and cytokines in wound healing. Wound Repair Regen. 2008;16(5):585-601.
30. Armstrong DG, Jude EB. The role of matrix metalloproteinases in wound healing. J Am Podiatr Med Assoc. 2002;92(1):12-8.
31. Kandhwal M, Behl T, Singh S, Sharma N, Arora S, Bhatia S, et al. Role of matrix metalloproteinase in wound healing. Am J Transl Res. 2022;14(7):4391-405.
32. Fukushima A, Yamaguchi T, Ishida W, Fukata K, Taniguchi T, Liu FT, et al. Genetic background determines susceptibility to experimental immune-mediated blepharoconjunctivitis: comparison of Balb/c and C57BL/6 mice. Exp Eye Res. 2006;82(2):210-8.
33. Wang Y, Zhang Y, Yang YP, Jin MY, Huang S, Zhuang ZM, et al. Versatile dopamine-functionalized hyaluronic acid-recombinant human collagen hydrogel promoting

diabetic wound healing via inflammation control and vascularization tissue regeneration. Bioact Mater. 2024;35:330-45.
34. Liu W, Gao R, Yang C, Feng Z, Ou-Yang W, Pan X, et al. ECM-mimetic immunomodulatory hydrogel for methicillin-resistant Staphylococcus aureus-infected chronic skin wound healing. Sci Adv. 2022;8(27):eabn7006.
35. He J, Chen J, Liu T, Qin F, Wei W. Research Progress of Multifunctional Hydrogels in Promoting Wound Healing of Diabetes. Int J Nanomedicine. 2025;20:7549-78.
36. Rubinstein MR, Genaro AM, Wald MR. Differential effect of hyperglycaemia on the immune response in an experimental model of diabetes in BALB/cByJ and C57Bl/6J mice: participation of oxidative stress. Clin Exp Immunol. 2013;171(3):319-29.
37. Huang C, Dong L, Zhao B, Lu Y, Huang S, Yuan Z, et al. Anti-inflammatory hydrogel dressings and skin wound healing. Clinical and translational medicine. 2022;12(11):e1094.
38. Dąbrowska A, Spano F, Derler S, Adlhart C, Spencer ND, Rossi RM. The relationship between skin function, barrier properties, and body-dependent factors. Skin Research and Technology. 2018;24(2):165-74.
39. Hu P, Yang Q, Wang Q, Shi C, Wang D, Armato U, et al. Mesenchymal stromal cells-exosomes: a promising cell-free therapeutic tool for wound healing and cutaneous regeneration. Burns & trauma. 2019;7.
40. Rahimnejad M, Derakhshanfar S, Zhong W. Biomaterials and tissue engineering for scar management in wound care. Burns & trauma. 2017;5.
41. Murray RZ, West ZE, Cowin AJ, Farrugia BL. Development and use of biomaterials as wound healing therapies. Burns & trauma. 2019;7.
42. Tehrany PM, Rahmanian P, Rezaee A, Ranjbarpazuki G, Sohrabi Fard F, Asadollah Salmanpour Y, et al. Multifunctional and theranostic hydrogels for wound healing acceleration: An emphasis on diabetic-related chronic wounds. Environ Res. 2023;238(Pt 1):117087.
43. Bowler PG. Wound pathophysiology, infection and therapeutic options. Ann Med. 2002;34(6):419-27.
44. Zaman SB, Hussain MA, Nye R, Mehta V, Mamun KT, Hossain N. A Review on Antibiotic Resistance: Alarm Bells are Ringing. Cureus. 2017;9(6):e1403.
45. Cristea Hohota AG, Lisa EL, Iacob Ciobotaru S, Dragostin I, Stefan CS, Fulga I, et al. Antimicrobial Smart Dressings for Combating Antibiotic Resistance in Wound Care. Pharmaceuticals (Basel). 2025;18(6).
46. Villalba-Rodríguez AM, Martínez-González S, Sosa-Hernández JE, Parra-Saldívar R, Bilal M, Iqbal HM. Nanoclay/polymer-based hydrogels and enzyme-loaded nanostructures for wound healing applications. Gels. 2021;7(2):59.
47. Yao H, Wu M, Lin L, Wu Z, Bae M, Park S, et al. Design strategies for adhesive hydrogels with natural antibacterial agents as wound dressings: Status and trends. Materials Today Bio. 2022;16:100429.
48. Herianto S, Hou CY, Lin CM, Chen HL. Nonthermal plasma-activated water: A comprehensive review of this new tool for enhanced food safety and quality. Comprehensive Reviews in Food Science and Food Safety. 2021;20(1):583-626.
49. Rathore V, Nema SK. Optimization of process parameters to generate plasma activated water and study of physicochemical properties of plasma activated solutions at optimum condition. Journal of Applied Physics. 2021;129(8).

50. Hoeben W, Van Ooij P, Schram D, Huiskamp T, Pemen A, Lukeš P. On the possibilities of straightforward characterization of plasma activated water. Plasma Chemistry and Plasma Processing. 2019;39(3):597-626.
51. Punith N, Harsha R, Lakshminarayana R, Hemanth M, S Anand M, Dasappa S. Plasma activated water generation and its application in agriculture. Advanced Materials Letters. 2019;10(10):700-4.
52. Machala Z, Tarabová B, Sersenová D, Janda M, Hensel K. Chemical and antibacterial effects of plasma activated water: Correlation with gaseous and aqueous reactive oxygen and nitrogen species, plasma sources and air flow conditions. Journal of Physics D: Applied Physics. 2018;52(3):034002.
53. Mao Y, Ma J, Xia Y, Xie X. The Overexpression of Epidermal Growth Factor (EGF) in HaCaT Cells Promotes the Proliferation, Migration, Invasion and Transdifferentiation to Epidermal Stem Cell Immunophenotyping of Adipose-Derived Stem Cells (ADSCs). Int J Stem Cells. 2020;13(1):93-103.
54. Saaristo A, Tammela T, Farkkila A, Karkkainen M, Suominen E, Yla-Herttuala S, et al. Vascular endothelial growth factor-C accelerates diabetic wound healing. Am J Pathol. 2006;169(3):1080-7.
55. Teller P, White TK. The physiology of wound healing: injury through maturation. Surg Clin North Am. 2009;89(3):599-610.
56. Merkulova Y, Shen Y, Parkinson LG, Raithatha SA, Zhao H, Westendorf K, et al. Granzyme B inhibits keratinocyte migration by disrupting epidermal growth factor receptor (EGFR)-mediated signaling. Biol Chem. 2016;397(9):883-95.
57. Qi X, Cai E, Xiang Y, Zhang C, Ge X, Wang J, et al. An Immunomodulatory Hydrogel by Hyperthermia-Assisted Self-Cascade Glucose Depletion and ROS Scavenging for Diabetic Foot Ulcer Wound Therapeutics. Adv Mater. 2023;35(48):e2306632.
58. Cao J, Wu B, Yuan P, Liu Y, Hu C. Rational Design of Multifunctional Hydrogels for Wound Repair. J Funct Biomater. 2023;14(11).
59. Peng Y, Guo Y, Ge X, Gong Y, Wang Y, Ou Z, et al. Construction of programmed time-released multifunctional hydrogel with antibacterial and anti-inflammatory properties for impaired wound healing. J Nanobiotechnology. 2024;22(1):126.